THE JOURNAL OF BIOLOGICAL CHEMISTRY VOL. 285, NO. 50, pp. 39171–39179, December 10, 2010

Impaired Orai1-mediated Resting Ca^{2+} Entry Reduces the Cytosolic $[Ca^{2+}]$ and Sarcoplasmic Reticulum Ca^{2+} Loading in Quiescent Junctophilin 1 Knock-out Myotubes*

Received for publication, May 29, 2010, and in revised form, September 29, 2010 Published, JBC Papers in Press, October 11, 2010, DOI 10.1074/jbc.M110.149690

Hongli Li[‡1], **Xudong Ding**[‡2], **Jose R. Lopez**[‡], **Hiroshi Takeshima**[§], **Jianjie Ma**[¶], **Paul D. Allen**[‡], **and Jose M. Eltit**[‡3]

From the [‡]*Department of Anesthesiology Perioperative and Pain Medicine, Brigham & Women's Hospital, Boston, Massachusetts 02115, the* [§]*Department of Biological Chemistry, Graduate School of Pharmaceutical Sciences, Kyoto University, Kyoto 606-8501, Japan, and the* [¶]*Department of Physiology and Biophysics, Robert Wood Johnson Medical School, Piscataway, New Jersey 08854*

In the absence of store depletion, plasmalemmal Ca^{2+} permeability in resting muscle is very low, and its contribution in the maintenance of Ca^{2+} homeostasis at rest has not been studied in detail. Junctophilin 1 knock-out myotubes (JP1 KO) have a severe reduction in store-operated Ca^{2+} entry, presumably caused by physical alteration of the sarcoplasmic reticulum (SR) and T-tubule junction, leading to disruption of the SR signal sent by Stim1 to activate Orai1. Using JP1 KO myotubes as a model, we assessed the contribution of the Orai1-mediated Ca^{2+} entry pathway on overall Ca^{2+} homeostasis at rest with no store depletion. JP1 KO myotubes have decreased Ca^{2+} entry, $[Ca^{2+}]_{rest}$, and intracellular Ca^{2+} content compared with WT myotubes and unlike WT myotubes, are refractory to BTP2, a Ca^{2+} entry blocker. JP1 KO myotubes show down-regulation of Orai1 and Stim1 proteins, suggesting that this pathway may be important in the control of resting Ca^{2+} homeostasis. WT myotubes stably transduced with Orai1(E190Q) had similar alterations in their resting Ca^{2+} homeostasis as JP1 KO myotubes and were also unresponsive to BTP2. JP1 KO cells show decreased expression of TRPC1 and -3 but overexpress TRPC4 and -6; on the other hand, the TRPC expression profile in Orai1(E190Q) myotubes was comparable with WT. These data suggest that an important fraction of resting plasmalemmal Ca^{2+} permeability is mediated by the Orai1 pathway, which contributes to the control of $[Ca^{2+}]_{rest}$ and resting Ca^{2+} stores and that this pathway is defective in JP1 KO myotubes.

In muscle fibers and cultured myotubes, the free cytosolic Ca^{2+} concentration at rest ($[Ca^{2+}]_{rest}$) is strictly held at a low and narrow range (115 to 125 nM at room temperature) (1, 2). At the same time, the Ca^{2+} concentration in internal stores and the extracellular space is 10,000 times greater. To achieve this equilibrium, multiple mechanisms are working simultaneously to regulate basal Ca^{2+} levels.

At least three different mechanisms have been identified to preserve $[Ca^{2+}]_{rest}$ in skeletal muscle: (i) a highly abundant sarcoplasmic/endoplasmic reticulum Ca^{2+} ATPase (SERCA)[4] that recaptures Ca^{2+} into the SR, (ii) the sarcolemmal Na^+/Ca^{2+} exchanger, which has a low Ca^{2+} affinity but high transporter capacity to remove Ca^{2+} from the cytoplasm to the extracellular space, and (iii), the plasma membrane Ca^{2+} ATPase, which transports Ca^{2+} from the cytoplasm to the extracellular space with a Ca^{2+} high affinity but low capacity. Although the first mechanism is most important in the short term, the latter two are critical for long term control. In addition to these "classical" regulatory mechanisms, there is ample evidence for a passive efflux of Ca^{2+} from the SR (Ca^{2+} leaks) through the ryanodine-insensitive pathway that also significantly contribute to regulation of $[Ca^{2+}]_{rest}$ in skeletal muscle (3).

Despite the strong electrochemical potential that Ca^{2+} ions have toward the intracellular space at rest, resting Ca^{2+} entry (R_{CaE}) is barely detectable due to the virtual impermeability of the cell membrane to Ca^{2+}, and this observation would suggest that extracellular Ca^{2+} permeability does not contribute to setting $[Ca^{2+}]_{rest}$. However, against this suggestion is the fact that a brief removal of extracellular Ca^{2+} has been shown to cause a decrease of $[Ca^{2+}]_{rest}$ in adult skeletal muscle (4). The mechanisms that control Ca^{2+} entry in muscle cells at rest are not well identified. What is known is that the acute depletion of the intracellular Ca^{2+} stores, using SERCA inhibitors, results in an increased permeability to extracellular Ca^{2+} (SOCE) (5, 6). One of the molecular determinants of this phenomenon is Stim1 (stromal interaction molecule 1), which acts as an intraluminal Ca^{2+} sensor of the SR (7, 8). The high luminal $[Ca^{+2}]$ in the SR at rest prevents oligomerization of Stim1 monomers, but when luminal $[Ca^{2+}]$ is lowered, it promotes Stim1 oligomerization and clustering of Stim1 in the endoplasmic reticulum/SR. While in this conformation, Stim1 interacts with Orai1, which is an integral pro-

* This work was supported, in whole or in part, by National Institutes of Health/NIAMS Grants 2R01AR43140 (to P. D. A.), RO1AG28856 (to J. M. and H. T.), and RO1HL69000 (to J. M.).

[1] Present address: Dept. of Histology and Embryology, Third Military Medical University, Chongqing 400038, China.

[2] Present address: Dept. of Anesthesia, Shengjing Hospital, China Medical University, Liaoning 110004, China.

[3] To whom correspondence should be addressed: Dept. of Anesthesiology Perioperative and Pain Medicine, Brigham and Women's Hospital, 75 Francis St., Boston, MA 02115. E-mail: jmeltit@zeus.bwh.harvard.edu.

[4] The abbreviations used are: SERCA, sarcoplasmic/endoplasmic reticulum Ca^{2+} ATPase; SOCE, store-operated Ca^{2+} entry; JP1 KO, junctophilin 1 knock-out; SR, sarcoplasmic reticulum; R_{CaE}, resting Ca^{2+} entry; TRPC, canonical transient receptor potential; f.a.u., fluorescence arbitrary units; ANOVA, analysis of variance; NS, no significant difference; RyR1, ryanodine receptor; OAG, 1-oleoyl-2-acetylglycerol.

tein of the plasma membrane (9–11). Support for the interaction of Stim1 and Orai1 being one mechanism for SOCE is found from experiments that show that Orai1 knock-out/knockdown or the expression of dominant negative forms of Orai1 almost completely prevents SOCE despite normal clustering of Stim1 (10–12). Although it has been proposed that Orai1 by itself could be the Ca^{2+} channel responsible for the SOCE current, the participation of canonical transient receptor potential (TRPC) channels alone or in concert with Orai1 in this process has also been suggested (13–16). In immortal cell lines, it has been shown that an Orai1-dependent mechanism orchestrated with a Ca^{2+} store sensor works as a feedback loop, which might contribute to keep $[Ca^{2+}]_{rest}$ and the SR Ca^{2+} stores at normal levels, suggesting a link between SOCE and the control of the resting Ca^{2+} homeostasis (17).

The membrane system of skeletal muscle is highly organized in triads where the junctional SR and the T-tubule membrane are only ~10 nm apart. The proximity of these two membranes is critical for the physical coupling between the dihydropyridine receptor and the ryanodine receptor 1 (RyR1) for EC coupling and likewise for the coupling of Stim1 and Orai1 for SOCE (18). Orai1 and several TRPC channels (TRPC1, -2, -3, -4 and -6) are expressed in skeletal muscle as well as in cultured myotubes (18–20), and most of these channels have been localized in or near the triad junction. It is believed that junctophilins (JP1 and JP2) are the specialized proteins in the triad that maintain the proper spatial disposition of the triad membranes (21–23). Decreased expression of JP proteins by knockdown/knock-out strategies has been shown to cause altered triad formation, and this structural alteration is thought to be responsible for the decreased SOCE found in JP1 KO muscle cells (23). However, the mechanism by which the absence of JP1 affects SOCE other than the presumed association with this structural change has not been investigated.

In the current study, we explored the possible failure of Orai1-mediated sarcolemmal Ca^{+2} entry at rest and the concomitant alterations in the resting Ca^{+2} homeostasis in JP1 KO skeletal myotubes. Using the Ca^{2+} entry blocker BTP2 and Orai1 pore mutant (E190Q), we demonstrated that an Orai1-mediated entry pathway at rest is blocked by BTP2 and that this pathway is absent in JP1 KO myotubes. In addition, we show that the Orai1-dependent R_{CaE} is fundamental to maintain levels of physiological $[Ca^{2+}]_{rest}$ in the cytosol and to maintain the Ca^{2+} content in intracellular stores.

EXPERIMENTAL PROCEDURES

Cell Culture—WT or JP1 KO myoblasts were plated either on 96-well imaging plates or 35-mm plates in Ham's F-10 medium (Invitrogen) supplemented with 20% bovine growth serum and 5 ng/ml basic fibroblast growth factor (Thermo Fisher Scientific). The following day, differentiation was started by changing the media to DMEM (Invitrogen) supplemented with 2% heat inactivated horse serum (Sigma).

Permanent Expression of Orai1 and Orai1(E190Q) in Myoblasts—Orai1 and Orai1(E190Q) cDNAs cloned into a retroviral expression vector with a bicistronic eGFP expression cassette and puromycin resistance were obtained from Addgene (Cambridge, MA, plasmids 12199 and 21662, respectively). These plasmids were kindly deposited by Dr. Anjana Rao (Harvard Medical School and Immune Disease Institute, Boston, MA) (11). We verified the correct sequence of both inserts and retroviral particles were packaged in HEK 293 helper cells, and myoblasts were infected with either construct at a multiplicity of infection of 5. Cells were allowed to recover for 12 h and then selected with puromycin (0.5 μg/ml) for 1 week. After the selection period, all remaining cells on the plate show the expression of the eGFP marker. An uninfected cell culture did not survive to the selection protocol, and wild type cells were used as controls.

Double-barreled Ca^{2+} Microelectrodes and $[Ca^{2+}]_{rest}$ Measurements—Double-barreled Ca^{2+}-selective microelectrodes were prepared using thin-walled borosilicate glass capillaries with filament (PB150F-4, World Precision Instruments, Sarasota, FL) as described previously (2). They were back-filled first with the neutral carrier ETH 129 (21193 Fluka-Sigma-Aldrich) and then with *p*Ca 7 solution. Each Ca^{2+}-selective microelectrode was individually calibrated as described previously (4), and only those with a linear relationship between *p*Ca 3 and *p*Ca 7 (Nernstian response, 28.5 mV per *p*Ca unit) were used experimentally. After making measurements of resting $[Ca^{2+}]$, all electrodes were then recalibrated, and if the two calibration curves did not agree within 3 mV, data from that microelectrode were discarded. Before starting the studies, we determined by direct calibration that the Ca^{2+} sensitivity of Ca^{2+} microelectrodes was not affected by any of the drugs used in the present study.

Microelectrode recordings were performed as described previously (2). Single myotubes were impaled with the double-barreled Ca^{2+}-selective microelectrode, and the potentials were recorded via high impedance amplifier (Duo 773 electrometer, World Precision Instruments, Sarasota, FL). The potential from the 3 M KCl microelectrode (V_m) was subtracted electronically from the potential of the Ca^{2+} electrode (V_{CaE}), to produce a differential Ca^{2+}-specific potential (V_{Ca}) that represents $[Ca^{2+}]_{rest}$. V_m and V_{Ca} were filtered (30–50 KHz) to improve the signal-to-noise ratio and stored in a computer for further analysis.

Store-operated Ca^{2+} Entry Measurements—5 to 6 days after differentiation, the myotubes were loaded with 5 μM Fura2-AM (Invitrogen) for 30 min at 37 °C. After three washes with imaging solution (140 mM NaCl, 5 mM KCl, 1 mM $MgCl_2$, 1 mM $CaCl_2$, 5,5 mM glucose, 10 mM Hepes, pH 7.4), the cells were subjected to a Ca^{2+} store depletion protocol, incubating the cells in zero Ca^{2+} solution (140 mM NaCl, 5 mM KCl, 2 mM $MgCl_2$, 5,5 mM glucose, 1 mM EGTA, 10 mM Hepes, pH 7.4) supplemented with 5 μM thapsigargin. After 20 min, the cells were placed on the stage of a TE2000 epifluorescence microscope (Nikon) coupled to a digital acquisition system (Stanford Photonics, Stanford CA). The cells were illuminated at the isosbestic Fura2 excitation wavelength (360 nm), and the fluorescence was measured at 510 nm. Cells were then perfused with zero Ca^{2+} solution and after 30 s switched to Mn^{2+}-containing solution (140 mM NaCl, 5 mM KCl, 0.5 mM $MnCl_2$, 5.5 mM glucose, 10 mM Hepes, pH 7.4), and the changes in Fura2 fluorescence were monitored.

Resting Ca^{2+} Entry Measurements—Fura2-loaded myotubes were perfused with imaging solution for 1 min, and then the perfusion system switched to Mn^{2+}- containing solution for 3 min. Some recordings showed motion artifact due to perfusion switching and to minimize errors in calculating the rate of decrease in Fura2 fluorescence after Mn^{2+} exposure, the rate was measured when the signal was linear and stable (30 s after solution twitching). To calculate the fluorescence quench rate, the stable part of the signal was fitted to a linear regression ($y = a + bx$). The slope derived is expressed as fluorescence arbitrary units (f.a.u.) per second.

Western Blot Analysis—Membrane vesicle preparation and immunoblotting were prepared from differentiated myotubes. The cells were homogenized in a Polytron cell disrupter in 5 mM imidazole, pH 7.4, 300 mM sucrose supplemented with protease inhibitor (Complete™, Roche Applied Science) and collected as described previously (24). Proteins were separated using SDS-PAGE and transferred to polyvinylidene difluoride membranes. Expression of specific proteins was assessed by incubation of the membranes with poly- or monoclonal antibodies against junctophilin 1 (Zymed Laboratories Inc., San Francisco, CA); junctophilin 2 (Zymed Laboratories Inc., San Francisco, CA); Stim1 (Affinity BioReagents, Golden, CO); Orai1 (AnaSpec, Inc., San Jose, CA); glyceraldehyde-3-phosphate dehydrogenase (FL-335, Santa Cruz Biotechnology, Santa Cruz, CA); TRPC1 (Santa Cruz Biotechnology); and TRPC3, TRPC4, and TRPC6 (Abnova, Walnut, CA).

Sarcoplasmic Reticulum Loading Capacity—Myotube preparations were loaded with 5 μM Fluo-4 AM for 30 min at 37 °C. The myotubes were placed on the stage of a Nikon TE2000 epifluorescence microscope coupled to a digital acquisition system (Stanford Photonics). A filter set with an excitation of 480/30 nm and emission of 535/40 nm was used. The emission signal was acquired at a frequency of 30 frames per second. The amount of SR Ca^{2+} was estimated by taking the combined area under the curve of three sequential exposures to 20 mM caffeine in Ca^{2+}-free medium to prevent Ca^{2+} entry to get the total area under the curve to assess the total amount of Ca^{2+} released. To estimate the total intracellular Ca^{2+} store, Fluo-4 AM-loaded myotubes were exposed to the Ca^{2+} ionophore 4Br-A23187 in Ca^{2+}-free medium. The area of the released Ca^{2+} was computed for each myotube type studied.

Statistics—All values are expressed as mean ± S.E., with the numbers in parentheses indicating the number of myotubes tested. Statistical analysis was performed using one-way analysis of variance and Tukey's test for multiple measurements to determine significance ($p < 0.05$).

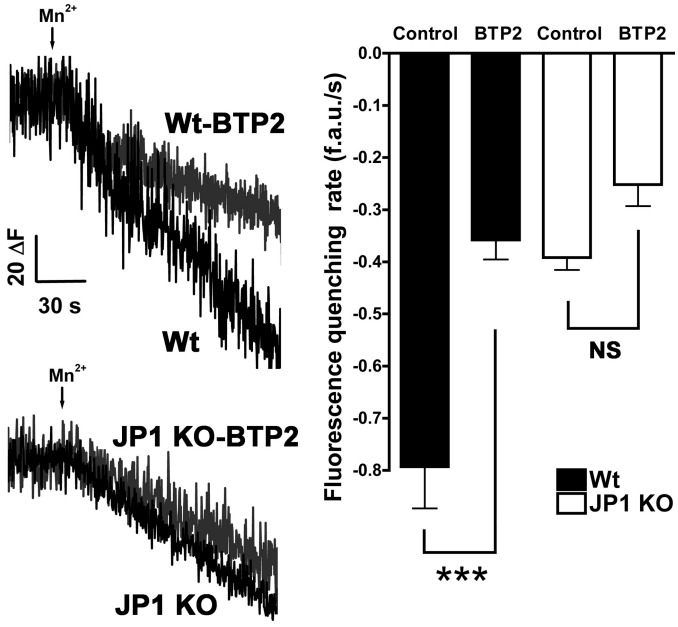

FIGURE 1. **Estimation of resting Ca^{2+} entry (R_{CaE}) in WT and JP1 KO myotubes.** R_{CaE} was estimated using the Mn^{2+} quench technique in myotubes that were not subjected to store depletion as described under "Experimental Procedures." The *arrow* shows the time point when the Mn^{2+}-containing solution was applied by the automatic perfusion system. The rate of fluorescence decay for each individual trace was calculated as the slope of a linear regression. WT and JP1 myotubes were tested in the presence and absence of 5 μM BTP2. Mean ± S.E. is plotted for each condition. ***, $p < 0.001$; one-way ANOVA.

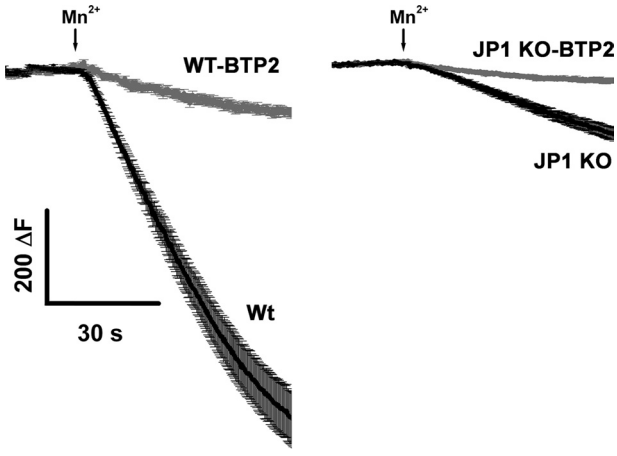

FIGURE 2. **SOCE in WT and JP1 KO myotubes.** SOCE was evaluated by a Mn^{2+} quench technique in myotubes subjected to store depletion as described under "Experimental Procedures." The *arrow* indicates the time point when the perfusion system was switched to a Mn^{2+}-containing solution. In the *left panel* are shown the SOCE signals of WT myotubes and the effect of 5 μM BTP2. The *right panel* shows Mn^{2+} entry in JP1 KO myotubes in the absence or presence of 5 μM BTP2. Mean traces ± S.E. of at least 20 myotubes are shown.

RESULTS

Effect of BTP2 on R_{CaE} and SOCE—Ca^{2+} influx at rest in WT myotubes measured using Mn^{2+} quench showed a slow decay in Fura2 fluorescence signal after Mn^{2+} exposure with a rate of −0.79 ± 0.08 (f.a.u)/s ($n = 61$). Incubation with BTP2 reduced the quench rate by more than half to −0.36 ± 0.04 (f.a.u)/s ($n = 38$). Interestingly, JP1 KO myotubes had a lower quench rate at rest than WT myotubes (−0.39 ± 0.02 (f.a.u)/s ($n = 87$)), and although BTP2 treatment decreased the rate to −0.25 ± 0.04 (f.a.u)/s ($n = 41$), this difference was not statistically significant (ANOVA analysis in Fig. 1) from untreated cells.

After a depletion protocol with thapsigargin, WT myotubes showed robust Mn^{2+} entry, which was strongly affected by 5 μM BTP2 (Fig. 2, *left*). In contrast, JP1 KO myotubes showed markedly decreased Mn^{2+} entry compared with WT myotubes; however, the small amount of Mn^{2+} entry that remained could also be blocked by BTP2 (Fig. 2, *right*).

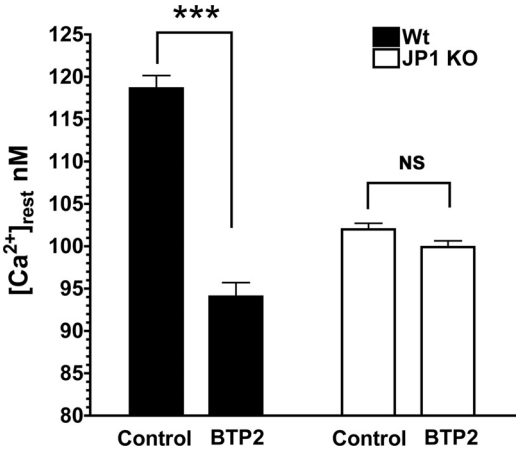

FIGURE 3. **Cytosolic free Ca^{2+} concentration at rest ($[Ca^{2+}]_{rest}$) in WT and JP1 KO myotubes.** $[Ca^{2+}]_{rest}$ was measured using calibrated Ca^{2+}-selective microelectrodes as described under "Experimental Procedures." The measurements were done in WT and JP1 KO myotubes under control conditions or exposed to 5 μM BTP2. Mean ± S.E. is plotted for each condition. ***, $p < 0.001$; one-way ANOVA.

BTP2 decreases $[Ca^{2+}]_{rest}$ in WT but Not in JP1 KO Myotubes—$[Ca^{2+}]_{rest}$ in WT myotubes was 118 ± 1.5 nM ($n = 19$) and 102 ± 0.7 nM, ($n = 12$) in JP1 KO myotubes ($p < 0.001$). In WT myotubes, exposure to 5 μM BTP2 for 10 min caused a reduction of $[Ca^{2+}]_{rest}$ to 94 ± 1.7 nM ($n = 19$) ($p < 0.01$). Similar treatment of JP1 KO myotubes with BTP2 had no effect on $[Ca^{2+}]_{rest}$ (100 ± 0.7 nM, $n = 10$, p = NS; Fig. 3).

BTP2 Treatment Partially Depletes Ca^{2+} Stores in WT Myotubes—To estimate the SR Ca^{2+} content in myotubes, we measured cytosolic Ca^{2+} transient induced by three consecutive 20 mM caffeine pulses in Ca^{2+}-free medium (Fig. 4, *A* and *B*), and the total integral of the three responses was computed. In WT myotubes, the integral was 3.2 ± 0.6 arbitrary units, ($n = 13$), and after treatment with BTP2, it was reduced to 1.3 ± 0.2 a.u. ($n = 16$, $p < 0.01$) (Fig. 4*C*). In JP1 KO myotubes, the integral was significantly lower than in WT cells (1.2 ± 0.2 a.u., $n = 30$, $p < 0.001$), but pretreatment with BTP2 had no effect on Ca^{2+} release in response to caffeine (1.1 ± 0.2 a.u., $n = 17$, p = NS, Fig. 4*C*). As a second approach to estimate the intracellular Ca^{2+} content, we exposed the myotubes to the Ca^{2+} ionophore 4Br-A23187 in Ca^{2+}-free medium (Fig. 4, *D* and *E*). The results were similar to those observed using caffeine. In WT cells, the Ca^{2+} release integral was 9.5 ± 0.9 a.u. ($n = 24$) before and 5.1 ± 0.5 a.u. ($n = 38$, $p < 0.001$) (Fig. 4*F*) after BTP2 treatment. In untreated JP1 KO myotubes, the Ca^{2+} integral was 4.6 ± 0.3 a.u. ($n = 52$; $p < 0.001$) and BTP2 treatment had no effect (4.0 ± 0.2 a.u., $n = 52$, p = NS, Fig. 4*F*).

Orai1 and Stim1 Expression Are Decreased in JP1 KO Myotubes—We evaluated the expression of two key proteins involved in Ca^{2+} entry, Stim1 and Orai1, in WT and JP1 KO myotubes. Western blot analysis shows that expression of both Orai1 and Stim1 are significantly decreased in JP1 KO cells (~65 and ~60% decrease, respectively, $n = 5$, $p < 0.01$), whereas the expression of JP2 remained unchanged (Fig. 5).

Expression of Orai1(E190Q) Decreases R_{CaE}, $[Ca^{2+}]_{rest}$, and SR Ca^{2+} Content at Rest—As was expected from previously published studies (12), the expression of the dominant negative form Orai1(E190Q) blocks SOCE in myotubes, whereas Orai1 overexpression does not have any effect (Fig. 6). In addition to the reduction of SOCE associated with overexpression of Orai1(E190Q), R_{CaE} was also significantly lower (−0.28 ± 0.02 (f.a.u./s), $n = 52$, $p < 0.01$) compared with Orai1-overexpressing myotubes (−0.58 ± 0.04 (f.a.u./s), $n = 46$; Fig. 7). After BTP2 pretreatment, the R_{CaE}, in Orai1-overexpressing myotubes, decreased to −0.31 ± 0.03 (f.a.u./s), $n = 39$ ($p < 0.001$), whereas in Orai1(E190Q), expressing cells were unresponsive to BTP2 (−0.26 ± 0.03 (f.a.u./s), $n = 39$ (p = NS)). In myotubes overexpressing Orai1, $[Ca^{2+}]_{rest}$ was 119 ± 0.6 nM ($n = 20$), and the addition of BTP2 reduces the $[Ca^{2+}]_{rest}$ to 95 ± 1.2 nM ($n = 10$, $p < 0.001$). In Orai1(E190Q) myotubes, the $[Ca^{2+}]_{rest}$ was 102 ± 1.2 nM ($n = 20$, $p < 0.001$, Fig. 7, *right panel*) and are refractory to BTP2 treatment ($[Ca^{2+}]_{rest}$ 102 ± 1.9 nM, $n = 11$, p = NS, Fig. 7, *right panel*).

The decrease in $[Ca^{2+}]_{rest}$ in myotubes expressing Orai1(E190Q) was accompanied by a significant decrease in total internal store Ca^{2+} content as demonstrated in a drop in the Ca^{2+} integral after exposure to 4Br-A23187 in Ca^{2+}-free media to 6.6 ± 0.3 a.u. ($n = 54$, $p < 0.001$) compared with 8.7 ± 0.4 a.u. ($n = 82$) in Orai1-overexpressing myotubes (Fig. 8). BTP2 treatment decreases the total internal store Ca^{2+} content to 4.8 ± 0.2 a.u. ($n = 69$, $p < 0.001$) in Orai1-overexpressing myotubes, but BTP2 had no effect in myotubes expressing Orai1(E190Q) 6.4 ± 0.3 a.u. ($n = 53$, p = NS).

Western Blot Analyses Performed to Determine Levels of TRPC1, -3, -4, and -6 Expression in WT, JP1 KO, Orai1-overexpressing, and Orai1(E190Q)-expressing Myotubes—In JP1 KO myotubes, TRPC1 (46 ± 5%, $n = 4$) and TRPC3 (21 ± 5%, $n = 4$) expression were significantly reduced, whereas expression of TRPC4 (152 ± 10%, $n = 4$) and TRPC6 (178 ± 9%, $n = 3$) were increased (Fig. 9). All values are expressed as % expression compared with WT myotubes. Orai1-overexpressing cells had a decrease in the expression of TRPC1 (58 ± 13%, $n = 4$), WT levels of TRPC4 (125 ± 10%, $n = 4$) expression and increased expression of both TRPC3 (170 ± 34%, $n = 4$) and TRPC6 (168 ± 22%, $n = 3$). Interestingly, TRPC expression in Orai1(E190Q)-expressing myotubes was similar to WT cells (TRPC1, 90 ± 24%, $n = 4$; TRPC3, 99 ± 15%, $n = 4$; TRPC4, 81 ± 6%, $n = 4$; TRPC6, 90 ± 14, $n = 3$).

DISCUSSION

The mechanisms that regulate the intracellular Ca^{2+} homeostasis in quiescent skeletal muscle are not fully understood. Under resting conditions, any overall passive inward flux from the extracellular space and leak from the SR is compensated by active efflux by the plasma membrane Ca^{2+} ATPase and Na^+/Ca^{2+} exchanger and Ca^{2+} pumping to the SR by SERCA (Fig. 10, *left*). Maintaining this equilibrium is essential because chronic Ca^{2+} overload would activate some of the intracellular proteases that can trigger apoptosis (25). On the other hand, the opposite scenario,

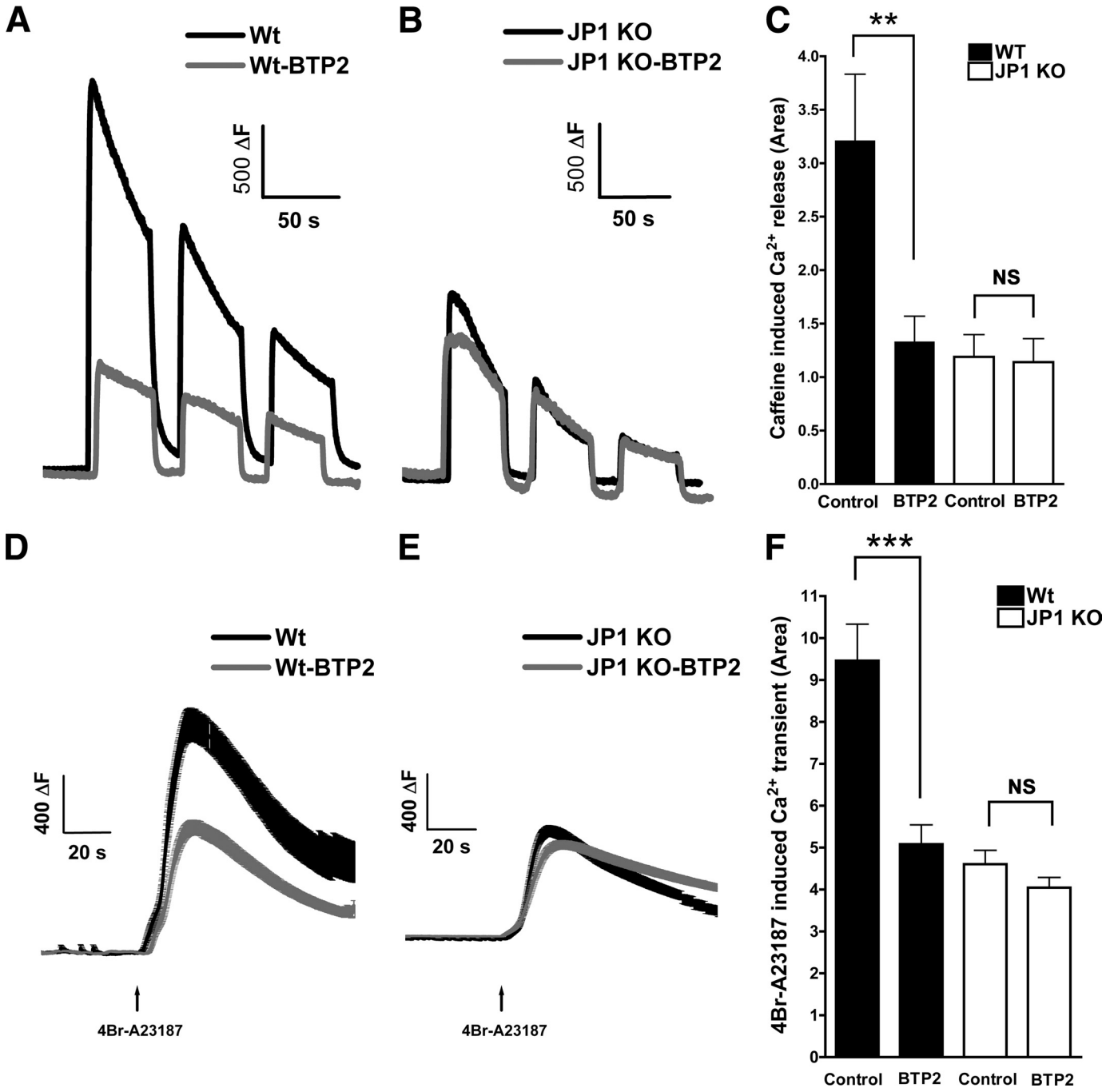

FIGURE 4. **Intracellular Ca^{2+} stores in WT and JP1 KO myotubes.** The amount of releasable SR Ca^{2+} was evaluated measuring the Ca^{2+} release induced by three consecutive pulses of 20 mM caffeine in Ca^{2+}-free solution as described under "Experimental Procedures." A representative response of WT (*A*) and JP1 KO (*B*) myotubes and the effect 5 μM BTP2 is shown. The integral of each response was calculated, and the total area was plotted (mean ± S.E.; *C*). ***, $p < 0.001$; one-way ANOVA. The intracellular Ca^{2+} content was evaluated measuring the Ca^{2+} release induced by the Ca^{2+} ionophore 4Br-A23187, in a Ca^{2+}-free solution as described under "Experimental Procedures." Mean traces ± S.E. of the Ca^{2+} release induced by 4Br-A23187 of WT (*D*) and JP1 KO myotubes (*E*) and the effect of 5 μM BTP2 is shown. The area under the curve of each response was calculated and plotted as mean ± S.E. (*F*). ***, $p < 0.001$; one-way ANOVA.

chronic Ca^{2+} depletion, could compromise muscle performance.

Hypothetically, to keep the perfect balance between influx and efflux, this system needs mechanisms to sense and modulate fluxes as is reflected in the stability of the actual values of $[Ca^{2+}]_{rest}$. However, the fact that a brief external Ca^{2+} withdraw is sufficient to affect $[Ca^{2+}]_{rest}$ suggests that mechanisms (SERCA, Na^+/Ca^{2+} exchanger, and plasma membrane Ca^{2+} ATPase) that have been indicated to be the major contributors are insufficient to explain how this can happen. Thus, it is clear that in addition to what been previously believed, other rapidly responding "on-line" mechanisms must be operating continuously at rest to set the proper $[Ca^{+2}]_{rest}$ and the correct loading in the SR.

In this study, we addressed the participation of extracellular Ca^{2+} influx at rest to maintain the proper $[Ca^{2+}]_{rest}$ in the

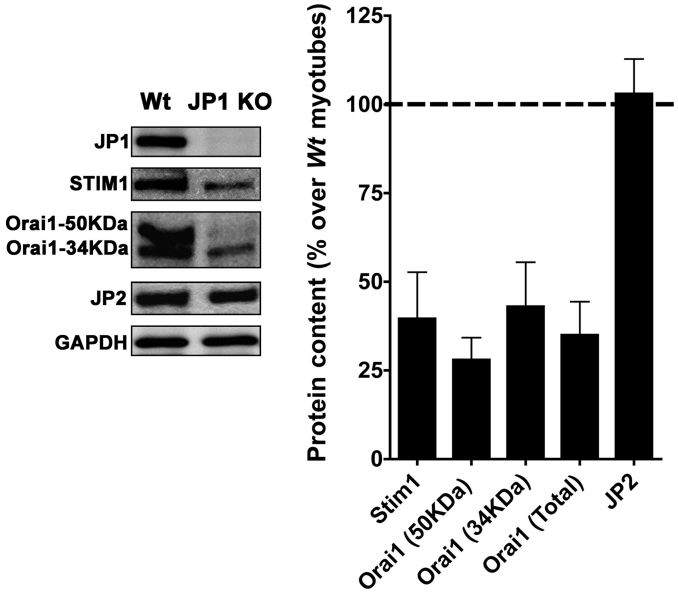

FIGURE 5. **Orai1 and Stim1 are dramatically decreased in JP1 KO myotubes.** Western blot analysis shows that the expression of Stim1, glycosylated Orai1 (50 kDa), and unglycosylated Orai1 (34 kDa) are strongly decreased in JP1 KO myotubes, whereas JP2 and GAPDH are unchanged compared with WT myotubes (*left panel*). A densitometric quantification of Western blot against the indicated proteins is shown. Each value was corrected with GAPDH band intensity as a loading correction, and the values are shown as % of the WT intensity (*right panel*). The *dashed line* shows the level of expression of WT myotubes.

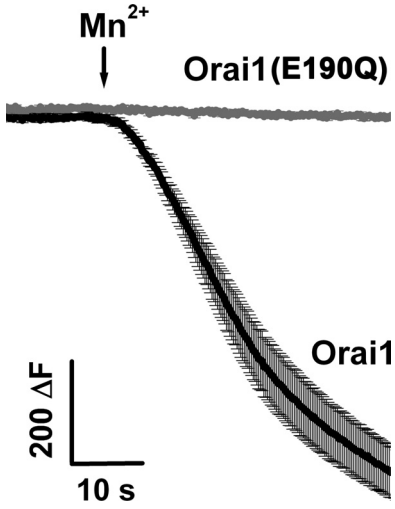

FIGURE 6. **SOCE in Orai1-defective myotubes.** SOCE was evaluated by a Mn^{2+} quench technique in myotubes subjected to store depletion as described under "Experimental Procedures." The *arrow* indicates the time point when the perfusion system was switched to Mn^{2+}-containing solution. SOCE signals of WT overexpressing Orai1 and WT myotubes expressing Orai1(E190Q) mutant are shown. Mean traces ± S.E. of at least 15 responses are plotted for each condition.

cytosol and in the SR. We used myotubes that lack the expression of JP1 protein, which has been proposed to be responsible for the interaction between the membranes of the triad junction. If this is the case, the lack of JP1 expression could affect the correct communication between proteins present in the SR membrane and proteins in the T-tubule, and this failure is the presumed explanation for the defect in SOCE demonstrated here and elsewhere (23) in JP1 KO myotubes. Thus, it was not surprising that our results showed that a reduction in SOCE in JP1 myotubes by >60% compared with WT myotubes was accompanied by a reduction in $[Ca^{2+}]_{rest}$.

To further characterize the contributors to the resting Ca^{2+} entry pathway, WT and JP1 KO myotubes were pretreated with BTP2, a cation entry blocker previously shown to block SOCE in T cells, DT40, and HEK293 cells (26, 27). The exact target of BTP2 is unclear, but it has been shown that it does not interfere with Ca^{2+} ATPase-coupled pumps, mitochondrial Ca^{2+} signaling, endoplasmic reticulum Ca^{2+} release, and K^+ channels in T cells (26). Incubation of myotubes with BTP2 blocks SOCE in WT cells and also eliminates the remaining SOCE in JP1-null myotubes.

In addition, it has been demonstrated that BTP2 blocks Sr^{2+} entry mediated by TRPC3 expressed in HEK cells when induced by activation of phospholipase C-coupled receptors using carbachol (27). Phospholipase C activation generates diacylglycerol, which is a known agonist of TRPC3 and TRPC6 channels (28). In addition, it has been shown that BTP2 blocks TRPC3 channels activated by the diacylglycerol analog OAG (27). BTP2 has also been shown to block Sr^{2+} entry through TRPC5 after carbachol stimulation (27), but as TRPC5 is not activated by diacylglycerol, this suggests that BTP2 is a general TRPC blocker regardless of the mechanism of activation.

The channels responsible of SOCE current in skeletal muscle are still controversial (18), but there is compelling data to suggest that Orai1/STIM1 are the major molecular components of SOCE in skeletal muscle (12, 19). BTP2 is very effective (IC_{50} = 0.1–0.3 μM) in blocking thapsigargin-induced Ca^{2+} entry (27). In this case, the BTP2 target is unknown. The finding that BTP2 "selectively" blocks iCRAC (Ca^{2+} release-activated Ca^{2+} current) in lymphocytes (26) and that both BTP2 and expression of the E190Q dominant negative form of Orai1 have a similar effect on SOCE and R_{CaE} in muscle cells strongly suggest that BTP2 acts on Orai1-mediated Ca^{2+} entry either directly or indirectly through an Orai1-TRPC channel complex rather than through a TRPC channel mechanism alone. Further investigation will be required to directly address the precise mechanism of action of BTP2 on Orai1 channel function.

A different outcome was obtained when we measured Mn^{2+} entry in cells that were not subjected to Ca^{2+} store depletion where the rate of entry was at least 20 times smaller than cells with empty Ca^{2+} stores. In WT myotubes, the estimated R_{CaE} was decreased by 50% by BTP2, suggesting an overlapping mechanism between SOCE and R_{CaE}. However, in JP1 KO myotubes, R_{CaE} is similar to that seen in WT myotubes exposed to BTP2, and further exposure of JP1 KO myotubes to BTP2 has a negligible effect. These data show for the first time that in WT, at least two independent mechanisms work in tandem to control the fine tuning of R_{CaE}: one that is sensitive to BTP2 and another that is refractory BTP2. On the other hand, in JP1 KO myotubes, the primary mechanism for Ca^{2+} entry is via the BTP2-insensitive pathway, whereas the role of the BTP2-sensitive pathway is almost insignificant. In addition, the BTP2-sensitive Ca^{2+} entry pathway is also responsible for fine tuning the Ca^{2+} content of SR, as demonstrated by the fact that JP1 KO myotubes and WT myotubes

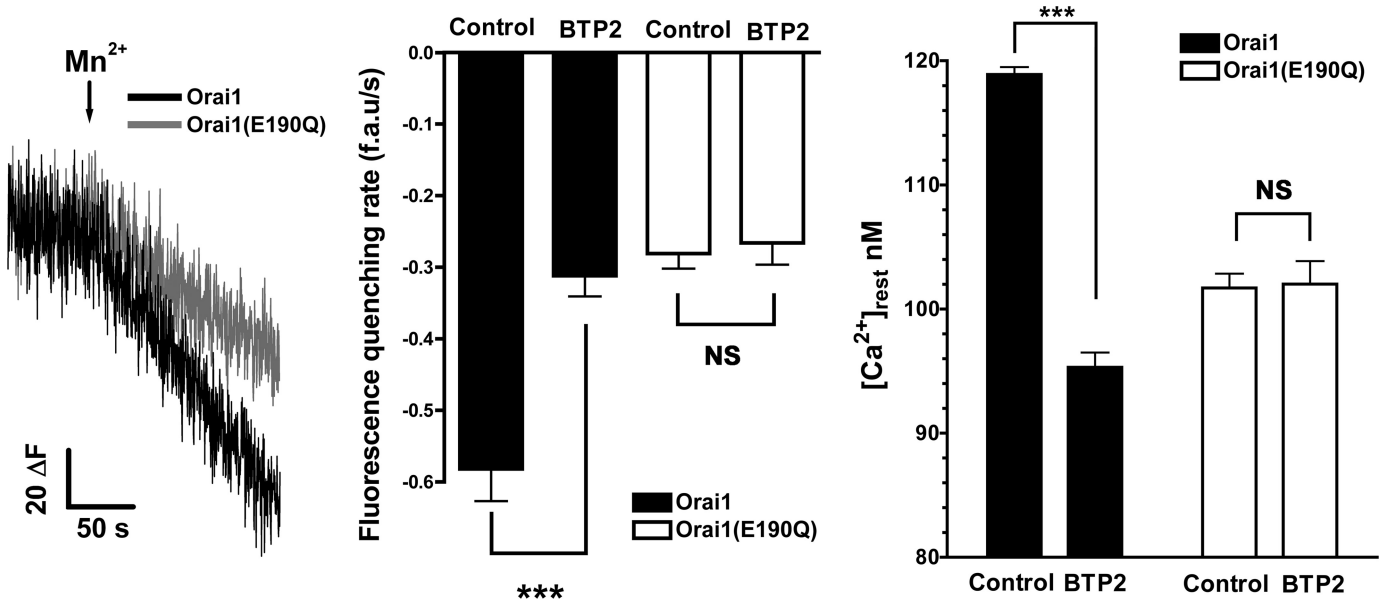

FIGURE 7. **Estimation of R_{CaE} and cytosolic free Ca^{2+} concentration at rest in Orai1-defective myotubes.** R_{CaE} was estimated using the Mn^{2+} quench technique in myotubes that were not subjected to store depletion as described under "Experimental Procedures." The *arrow* shows the time point when Mn^{2+}-containing solution was applied by the automatic perfusion system. Representative traces of WT overexpressing Orai1 and WT myotubes expressing Orai1(E190Q) mutant are shown (*left panel*). The rate of fluorescence decay for each individual trace was calculated as the slope of a linear regression. The slope of individual experiments were plotted as mean ± S.E. (*middle panel*). The effect of BTP2 treatment is shown. ***, $p < 0.001$; one way ANOVA. $[Ca^{2+}]_{rest}$ was measured using calibrated Ca^{2+}-selective microelectrodes as described under "Experimental Procedures." The measurements were done in WT overexpressing Orai1 or Orai1(E190Q) (*right panel*). Mean ± S.E. are plotted for each condition. ***, $p < 0.001$. The control condition and the effect of 5 μM BTP2 are shown.

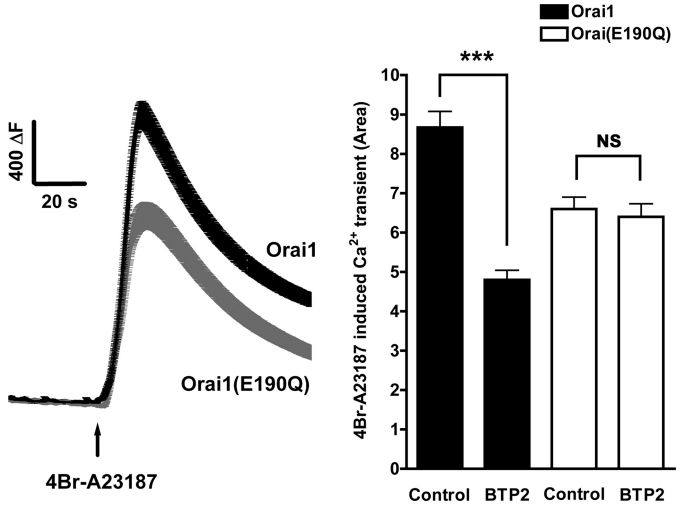

FIGURE 8. **Intracellular Ca^{2+} Stores in Orai1-defective WT myotubes.** The intracellular Ca^{2+} content was evaluated measuring the Ca^{2+} release induced by the Ca^{2+} ionophore 4Br-A23187 in a Ca^{2+}-free solution as described under "Experimental Procedures." Mean traces ± S.E. of the Ca^{2+} release induced by 4Br-A23187 of WT myotubes overexpressing Orai1 or Orai1(E190Q) are shown (*left panel*). The area under the curve of each response was calculated and plotted as mean ± S.E. (*right panel*); the effect of BTP2 treatment is shown, ***, $p < 0.001$.

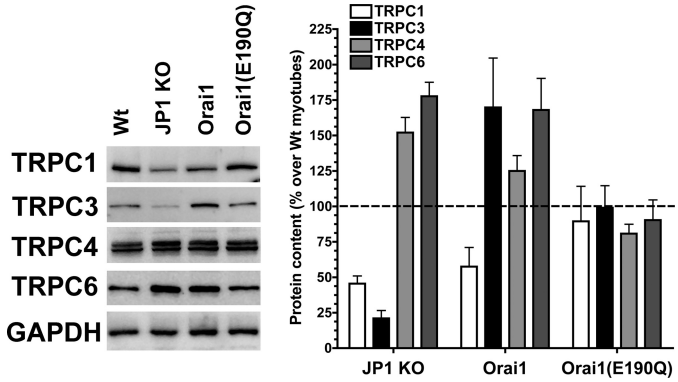

FIGURE 9. **TRPC1, -3, -4, and -6 expression in WT, JP1 KO, Orai1, and Orai1(E190Q) myotubes.** Western blot analysis shows the expression of TRPC1, TRPC3, TRPC4, and TRPC6 in WT, JP1 KO, Orai1, and Orai1(E190Q) myotubes (*left panel*). TRPC4 showed two bands that may correspond to splicing forms described previously (31). In this case, we measured both bands together as an estimation of total TRPC4 expression. Densitometric quantification of Western blots against the indicated proteins are shown; each value was corrected with GAPDH band intensity as a loading correction, and the mean ± S.E. of at least three independent experiments are shown as % of the WT intensity (*right panel*). The *dashed line* shows the level of expression of WT myotubes.

pretreated with BTP2 have less Ca^{2+} in their stores than untreated WT myotubes.

Western blot analysis clearly shows a significant decrease of Orai1 and Stim1 protein levels in JP1 KO myotubes. This alteration itself could impair the regulatory feedback between Ca^{2+} stores in the SR and the permeability of the plasma membrane to Ca^{2+} both at rest and after store depletion. To test this hypothesis, we compared these results with those in cells that overexpressed the pore-defective E190Q Orai1 protein as a dominant negative in WT myotubes. Orai1(E190Q) completely blocks SOCE in cultured myotubes as was previously shown by Lyfenko and Dirksen (12). In addition, Orai1(E190Q) decreases R_{CaE}, the amount of Ca^{2+} in internal stores and myoplasmic $[Ca^{2+}]_{rest}$, mimicking the JP1 KO phenotype and that of WT myotubes after exposure to BTP2. More importantly, similar to what is seen in JP1 KO myotubes, BTP2 has no effect on reducing $[Ca^{2+}]_{rest}$, maintenance of internal stores, and R_{CaE} in Orai1(E190Q)-expressing myotubes. Thus, these data demonstrate that the BTP2-sensitive

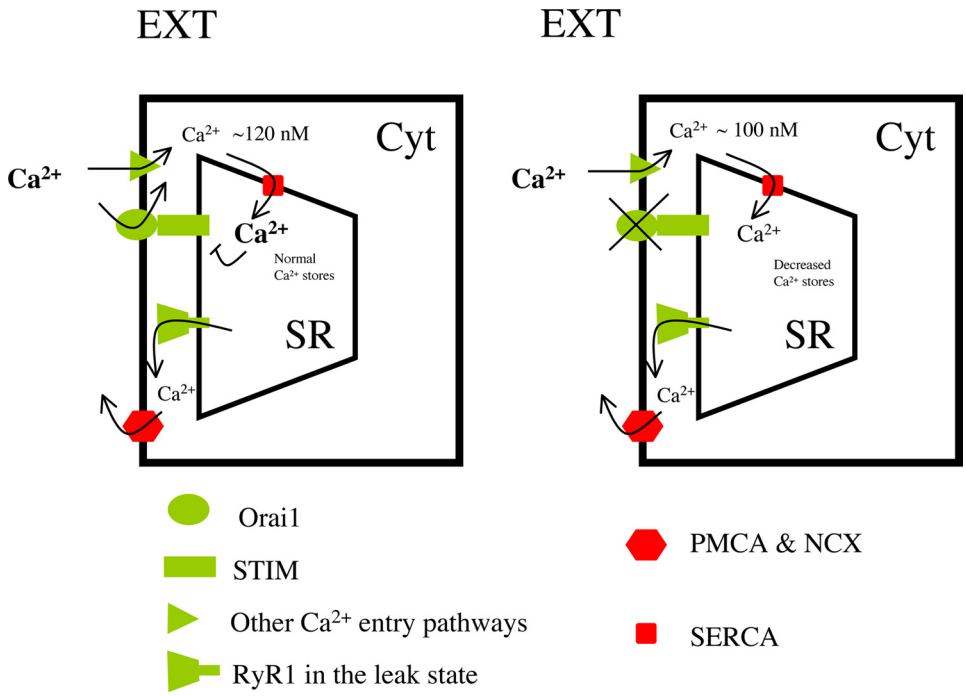

FIGURE 10. **Participation of Orai1 Ca^{2+} permeability in resting Ca^{2+} homeostasis in myotubes.** In resting conditions, the overall passive inward flux from the extracellular (*EXT*) space is compensated by active efflux. At the same time, Ca^{2+} that is pumped into the SR should be exactly the same to the Ca^{2+} that leaks from it, probably through the RyR1 in the leak state. All of these fluxes should be in equilibrium to reach a "normal" and constant [Ca^{2+}] in the cytosol (*Cyt*) and in internal stores (*left panel*). In resting conditions, at least two Ca^{2+} entry pathways are present in myotubes. One pathway involves the participation of Orai1, and the other is unknown. The ablation or defects of Orai1-mediated Ca^{2+} entry at rest result in an impaired control of the Ca^{+2} homeostasis in myotubes at rest, resulting in a decrease in $[Ca^{2+}]_{rest}$ and the SR Ca^{2+} content. This imbalance could be as a result of two phenomena the decreased Ca^{2+} influx and the lack of communication between the Ca^{2+} store levels and the extracellular Ca^{2+} permeability (*right panel*). *NCX*, Na^{+}/Ca^{2+} exchanger. *PMCA*, plasma membrane Ca^{2+} ATPase.

aspect of R_{CaE} at rest is dependant on Orai1 and suggests that the decreased expression of Orai1 in JP1 KO myotubes or blocking the Orai1-dependent fraction of the R_{CaE} by BTP2 in WT myotubes leads to altered resting Ca^{2+} homeostasis.

Since TRPCs are known targets of BTP2, the alternative hypothesis was that the unresponsiveness of JP1 KO as well as Orai1(E190Q) myotubes to BTP2 treatment was due to altered expression of TRPCs. Although TRPC1 and TRPC3 expression is reduced in JP1 KO myotubes compared with WT cells, the expression of TRPC4 and TRPC6 (which are similar in structure an function to TRPC1 and TRPC3, respectively (29, 30)) are compensatorily increased, suggesting that low expression of TRPC1 and TRPC3 is not the primary cause of BTP2 unresponsiveness. Furthermore, the fact that Orai1(E190Q)-expressing myotubes are refractory to BTP2 but have a TRPC expression profile that is almost identical to WT cells suggests that changes in TRPC expression cannot account for the alterations in resting Ca^{2+} homeostasis that we observed.

In a previous report (23), it was shown that in muscle fibers in which adenoviral-shRNA was used to knock down both JP1 and JP2 decreases both SOCE and SR Ca^{2+} content in agreement with this work. However, these results differ with our study in that a slight increase in the basal Fura2 F340/F360 ratio in muscle cells treated with shRNA compared with controls was found. At first, this last result could appear to be contradictory with the present work, but these results are not comparable because JP2 expression was not altered in the current study. The simultaneous knockdown of JP1 and JP2 proteins may cause additional alterations in Ca^{2+}-handling proteins that could shift the [Ca^{2+}] equilibrium at rest to higher levels in the cytosol, which could explain the previously observed small increase in resting Ca^{2+}. In addition, in the present study, calibrated microelectrodes were used, which is a much more precise and exact method to determine resting [Ca^{2+}]. These electrodes allow discrimination of differences in [Ca^{2+}] of <5 nM in the linear portion of the curve response (*p*Ca3–7), which gives further confidence that the differences that we observed are correct.

In summary, our data show that under resting conditions at least two Ca^{2+} entry pathways are present in myotubes. One of these pathways involves the participation of Orai1, which is sensitive to BTP2. The ablation of Orai1-mediated R_{CaE} results in an impaired control of the Ca^{+2} homeostasis in myotubes, resulting in a decrease in $[Ca^{2+}]_{rest}$ and SR Ca^{2+} content (Fig. 10, *right panel*).

REFERENCES

1. López, J. R., Contreras, J., Linares, N., and Allen, P. D. (2000) *Anesthesiology* **92,** 1799–1806
2. Yang, T., Esteve, E., Pessah, I. N., Molinski, T. F., Allen, P. D., and López, J. R. (2007) *Am. J. Physiol. Cell Physiol.* **292,** C1591–1598
3. Eltit, J. M., Yang, T., Li, H., Molinski, T. F., Pessah, I. N., Allen, P. D., and Lopez, J. R. (2010) *J. Biol. Chem.* **285,** 13781–13787
4. López, J. R., Alamo, L., Caputo, C., DiPolo, R., and Vergara, S. (1983) *Biophys. J.* **43,** 1–4
5. Kurebayashi, N., and Ogawa, Y. (2001) *J. Physiol.* **533,** 185–199
6. Pan, Z., Yang, D., Nagaraj, R. Y., Nosek, T. A., Nishi, M., Takeshima, H., Cheng, H., and Ma, J. (2002) *Nat. Cell Biol.* **4,** 379–383
7. Roos, J., DiGregorio, P. J., Yeromin, A. V., Ohlsen, K., Lioudyno, M.,

Zhang, S., Safrina, O., Kozak, J. A., Wagner, S. L., Cahalan, M. D., Veliçelebi, G., and Stauderman, K. A. (2005) *J. Cell Biol.* **169,** 435–445
8. Soboloff, J., Spassova, M. A., Tang, X. D., Hewavitharana, T., Xu, W., and Gill, D. L. (2006) *J. Biol. Chem.* **281,** 20661–20665
9. Feske, S., Gwack, Y., Prakriya, M., Srikanth, S., Puppel, S. H., Tanasa, B., Hogan, P. G., Lewis, R. S., Daly, M., and Rao, A. (2006) *Nature* **441,** 179–185
10. Vig, M., Peinelt, C., Beck, A., Koomoa, D. L., Rabah, D., Koblan-Huberson, M., Kraft, S., Turner, H., Fleig, A., Penner, R., and Kinet, J. P. (2006) *Science* **312,** 1220–1223
11. Prakriya, M., Feske, S., Gwack, Y., Srikanth, S., Rao, A., and Hogan, P. G. (2006) *Nature* **443,** 230–233
12. Lyfenko, A. D., and Dirksen, R. T. (2008) *J. Physiol.* **586,** 4815–4824
13. Liao, Y., Erxleben, C., Abramowitz, J., Flockerzi, V., Zhu, M. X., Armstrong, D. L., and Birnbaumer, L. (2008) *Proc. Natl. Acad. Sci. U.S.A.* **105,** 2895–2900
14. Liao, Y., Erxleben, C., Yildirim, E., Abramowitz, J., Armstrong, D. L., and Birnbaumer, L. (2007) *Proc. Natl. Acad. Sci. U.S.A.* **104,** 4682–4687
15. Yuan, J. P., Zeng, W., Huang, G. N., Worley, P. F., and Muallem, S. (2007) *Nat. Cell Biol.* **9,** 636–645
16. Ong, H. L., Cheng, K. T., Liu, X., Bandyopadhyay, B. C., Paria, B. C., Soboloff, J., Pani, B., Gwack, Y., Srikanth, S., Singh, B. B., Gill, D. L., Gill, D., and Ambudkar, I. S. (2007) *J. Biol. Chem.* **282,** 9105–9116
17. Brandman, O., Liou, J., Park, W. S., and Meyer, T. (2007) *Cell* **131,** 1327–1339
18. Shin, D. M., and Muallem, S. (2008) *Nat. Cell Biol.* **10,** 639–641
19. Stiber, J., Hawkins, A., Zhang, Z. S., Wang, S., Burch, J., Graham, V., Ward, C. C., Seth, M., Finch, E., Malouf, N., Williams, R. S., Eu, J. P., and Rosenberg, P. (2008) *Nat. Cell Biol.* **10,** 688–697
20. Vandebrouck, C., Martin, D., Colson-Van Schoor, M., Debaix, H., and Gailly, P. (2002) *J. Cell Biol.* **158,** 1089–1096
21. Ito, K., Komazaki, S., Sasamoto, K., Yoshida, M., Nishi, M., Kitamura, K., and Takeshima, H. (2001) *J. Cell Biol.* **154,** 1059–1067
22. Komazaki, S., Ito, K., Takeshima, H., and Nakamura, H. (2002) *FEBS Lett.* **524,** 225–229
23. Hirata, Y., Brotto, M., Weisleder, N., Chu, Y., Lin, P., Zhao, X., Thornton, A., Komazaki, S., Takeshima, H., Ma, J., and Pan, Z. (2006) *Biophys. J.* **90,** 4418–4427
24. Perez, C. F., López, J. R., and Allen, P. D. (2005) *Am. J. Physiol. Cell Physiol.* **288,** C640–649
25. MacLennan, D. H. (2000) *Eur. J. Biochem.* **267,** 5291–5297
26. Zitt, C., Strauss, B., Schwarz, E. C., Spaeth, N., Rast, G., Hatzelmann, A., and Hoth, M. (2004) *J. Biol. Chem.* **279,** 12427–12437
27. He, L. P., Hewavitharana, T., Soboloff, J., Spassova, M. A., and Gill, D. L. (2005) *J. Biol. Chem.* **280,** 10997–11006
28. Hofmann, T., Obukhov, A. G., Schaefer, M., Harteneck, C., Gudermann, T., and Schultz, G. (1999) *Nature* **397,** 259–263
29. Lee, K. P., Yuan, J. P., Hong, J. H., So, I., Worley, P. F., and Muallem, S. (2010) *FEBS Lett.* **584,** 2022–2027
30. Clapham, D. E., Julius, D., Montell, C., and Schultz, G. (2005) *Pharmacol. Rev.* **57,** 427–450
31. Mery, L., Magnino, F., Schmidt, K., Krause, K. H., and Dufour, J. F. (2001) *FEBS Lett.* **487,** 377–383